Title

Expansion of Dysfunctional Tim-3–Expressing Effector Memory CD8+ T Cells during Simian Immunodeficiency Virus Infection in Rhesus Macaques

Journal

The Journal of Immunology, 193(11)

ISSN

0022-1767

Authors

Fujita, Tsuyoshi
Burwitz, Benjamin J
Chew, Glen M
et al.

Publication Date

2014-12-01

DOI

10.4049/jimmunol.1400961

Peer reviewed

Published in final edited form as:
J Immunol. 2014 December 1; 193(11): 5576–5583. doi:10.4049/jimmunol.1400961.

Expansion of Dysfunctional Tim-3 Expressing Effector Memory CD8+ T cells during SIV Infection in Rhesus Macaques

Tsuyoshi Fujita[*,†,1], **Benjamin J. Burwitz**[‡,§,1], **Glen M. Chew**[*], **Jason S. Reed**[‡,§], **Reesab Pathak**[‡,§], **Elizabeth Seger**[‡,§], **Kiera L. Clayton**[¶], **James M. Rini**[¶], **Mario A. Ostrowski**[¶], **Naoto Ishii**[†], **Marcelo J Kuroda**[$], **Scott G. Hansen**[‡,§], **Jonah B. Sacha**[‡,§], and **Lishomwa C. Ndhlovu**[*]

[*]Hawaii Center for AIDS, Department of Tropical Medicine, University of Hawaii, John A. Burns School Medicine, Manoa, HI, USA

[†]Department of Microbiology and Immunology, Tohoku University Graduate School of Medicine, Sendai, Japan

[‡]Vaccine & Gene Therapy Institute, Oregon Health & Science University, Beaverton, OR, USA

[§]Oregon National Primate Research Center, Oregon Health & Science University, Beaverton, OR, USA

[¶]Department of Immunology, University of Toronto, Toronto, ON, Canada

[$]Division of Immunology, Tulane National Primate Research Center, 18703 Three Rivers Road, Covington LA, USA

Abstract

The T cell immunoglobulin- and mucin domain-containing molecule (Tim)-3 negative immune checkpoint receptor demarcates functionally exhausted $CD8^+$ T cells arising from chronic stimulation in viral infections like HIV. Tim-3 blockade leads to improved anti-viral $CD8^+$ T cell responses *in vitro* and therefore represents a novel intervention strategy to restore T cell function *in vivo* and protect from disease progression. However, the Tim-3 pathway in the physiologically relevant rhesus macaque SIV model of AIDS remains uncharacterized. We report here that $Tim\text{-}3^+CD8^+$ T cell frequencies are significantly increased in lymph nodes, but not in peripheral blood, in SIV-infected animals. $Tim\text{-}3^+PD\text{-}1^+CD8^+$ T cells are similarly increased during SIV infection and positively correlate with SIV plasma viremia. Tim-3 expression was found primarily on effector memory $CD8^+$ T cells in all tissues examined. $Tim\text{-}3^+CD8^+$ T cells have lower Ki-67 content and minimal cytokine responses to SIV compared to $Tim\text{-}3^-CD8^+$ T cells. During acute phase SIV replication Tim-3 expression peaked on SIV-specific $CD8^+$ T cells by 2 weeks post infection, and then rapidly diminished irrespective of mutational escape of cognate antigen,

Address correspondence and reprint requests to: Dr. Lishomwa C. Ndhlovu, MD, PhD. Hawaii Center for AIDS, Department of Tropical Medicine, University of Hawaii and John A. Burns School Medicine, Honolulu, HI 96813. Phone: 808-692-1604, lndhlovu@hawaii.edu or Dr. Jonah B. Sacha, PhD. Vaccine & Gene Therapy Institute and Oregon National Primate Research Center, Oregon Health & Science University, Beaverton, OR 97006. Phone: 503-418-2774, sacha@ohsu.edu.
[1]T.F. and B.J.B. are co-first authors and contributed equally to this work.

DISCLOSURES
The authors have no financial conflicts of interest.

suggesting non-TCR driven mechanisms for Tim-3 expression. Thus, rhesus Tim-3 in SIV infection partially mimics human Tim-3 in HIV infection and may serve as a novel model for targeted studies focused on rejuvenating HIV-specific $CD8^+$ T cell responses.

INTRODUCTION

Virus-specific $CD8^+$ T cells play a crucial role in the control of Simian immunodeficiency virus (SIV) and HIV infections (1-10). Recent studies demonstrate that effector memory $CD8^+$ T cells elicited by vaccination with SIV protein-expressing rhesus cytomegalovirus (RhCMV/SIV) vectors mediate stringent protection from SIV replication and can even clear latent SIV reservoirs (11, 12). Additionally, the magnitude and function of SIV-specific effector T cells are strongly associated with protection following live-attenuated SIV vaccination (13). These data indicate that the continuous generation and maintenance of robust effector memory HIV/SIV-specific $CD8^+$ T cells in peripheral tissues may afford a strategy for clearance of virus. Therefore, understanding T cell effector regulation is crucial to improving T-cell-based vaccine strategies.

Failure of the host immune system to control HIV/SIV infection is related, in part, to functional impairment of virus-specific $CD8^+$ T cells (14-22). In the presence of a high antigenic load, such as in chronic viral infections, T cells enter a state of exhaustion (23). During this period, T cells express several inhibitory immune receptors that fine-tune the strength of activating signals, resulting in negative feedback. While Programmed Death Receptor-1 (PD-1) is an early, sustained marker of immune exhaustion (14, 15, 18-22), recent studies have shown that the surface glycoprotein, T cell immunoglobulin- and mucin domain-containing molecule (Tim)-3, appears to be a later marker of T cell dysfunction, defined by defective proliferative capacity and cytokine production (16, 24-29). Our previous observations revealed that increased Tim-3 expression on HIV-specific $CD8^+$ T cells is associated with progressive HIV infection (25), and others have shown increased Tim-3 expression on $CD8^+$ T cells in patients with higher levels of HIV (30, 31) and HCV (17, 26, 32) infection. Additionally, it is evident from several studies that Tim-3^+CD8^+ T cells are an abundant, but entirely distinct and divergent population from prototypical anergic effector or memory $CD8^+$ T cells (33, 34).

Blockade of Tim-3 interaction, alone or in conjunction with PD-1 blocking, has been shown to reverse effector T cell defects, reduce viremia, and ameliorate disease severity in the setting of several chronic viral infections (15, 22, 24, 26, 27). Mechanistically, Tim-3 blockade allows Tim-3^+CD8^+ T cells to respond more efficiently to TCR stimulation (17, 25, 35), setting the stage for improved effector T cell responses.

The Tim-3 pathway in non-human primates has yet to be fully explored. Given the importance of non-human primates as models of human disease, understanding the similarities and differences between human and non-human primate Tim-3 signaling would provide additional avenues to study the therapeutic effects of Tim-3 blockade. In particular, non-human primates provide the most physiologically relevant model for HIV/AIDS. Therefore, we report here on the profile and characterization of Tim-3 expression in the peripheral blood and organized lymphoid tissues in SIV-infected rhesus macaques.

MATERIALS AND METHODS

Animals

Indian rhesus macaques (*Macaca mulatta*) housed at the Oregon National Primate Research Center (ONPRC) used in this study were cared for according to the laws, regulations, and guidelines set forth by the United States Department of Agriculture (e.g., the Animal Welfare Act and its regulations, and the Animal Care Policy Manual), Institute for Laboratory Animal Research (e.g., Guide for the Care and Use of Laboratory Animals, 8th edition), Public Health Service, National Research Council, Centers for Disease Control, and the Association for Assessment and Accreditation of Laboratory Animal Care (AAALAC) International. The Oregon Health and Science University Institutional Animal Care and Use Committee approved the research involving animals reported in this study. Animals were infected with SIVsmE660, SIVmac239, or SIVmac251 for other, unrelated projects.

Rhesus Tim-3 Cloning

Cryopreserved human and rhesus peripheral blood mononuclear cells (PBMC) were thawed and lysed and the RNA was purified using RNeasy Plus Mini Kit (Qiagen, Venlo, Limburg, Netherlands). Total RNA was reverse- transcribed with the Superscript III First- Strand Synthesis System (Invitrogen, Carlsbad, CA) using primers specific for Tim-3. RNA complimentary to the cDNA was removed using RNase H (Invitrogen). ExPASy translate tool was used to translate obtained DNA sequences to protein sequences. These sequence data are deposited at http://www.ddbj.nig.ac.jp with the accession number AB924452 (Human) and AB924453 (rhesus).

Western blot

Cryopreserved PBMC from HIV uninfected humans, SIV-uninfected and SIV-infected animals were thawed and lysed in radioimmunoassay precipitation (RIPA) buffer (Thermo Scientific, Waltham, MA) then incubated with PNGase F (New England BioLabs, Ipswich, MA). Samples were separated by 12% SDS-PAGE and blotted onto a nitrocellulose membrane (Amersham, Buckinghamshire, England). The membrane was blocked in 5% milk for an hour and incubated overnight with polyclonal goat anti-human Tim-3 antibody (R&D systems, Minneapolis, MN). Rabbit anti-goat HRP-conjugated antibody (Invitrogen) was used as a secondary antibody and then blots were developed by chemiluminescent method using ECL Prime Western Blotting Detection Reagent (Amersham).

Antibodies and flow cytometric analysis

The following directly conjugated antibodies were obtained from BD Bioscience, San Jose, CA: Alexa fluor 700-conjugated anti-CD3 (SP34-2), PE-CF594-conjugated anti-CD4 (L200), APC- or APC-H7-conjugated anti-CD8 (SK1), V450-conjugated anti-CD16 (3G8), PE-Cy7-conjugated anti-CD56 (NCAM16), PE-Cy5-conjugated anti-CD95 (DX2), APC-conjugated anti-IFN-γ (B27) and PE-conjugated anti-Ki-67 (B56). PE-conjugated anti-PD-1 (EH12.2H7), PE-Cy7-conjugated CD28 (CD28.2), and Alexa Flour 488-conjugated anti-Rabbit IgG (H+L) antibodies were purchased from BioLegend, San Diego, CA, from eBioscience, San Diego, CA, and from Invitrogen, respectively. Unconjugated Tim-3

polyclonal antibodies (from Life BioScience, Albuquerque, NM and Novus Biologicals, Littleton, CO) were used in concert with Alexa Flour 488-conjugated anti-Rabbit IgG (H+L) antibody. A biotinylated anti-human Tim-3 polyclonal antibody and biotinylated Goat polyclonal antibodies (R&D System) were used in concert with Qdot605-conjugated streptavidin (Invitrogen). PE-conjugated Tim-3 monoclonal antibodies were obtained from R&D (215008 and 344823) and BioLegend (F38-2E2). APC-conjugated Mamu-A*01 SIV $Gag_{181-189}$CM9 (CTPYDINQM) tetramer and APC-conjugated Mamu-A*01 SIV Tat_{28-35}SL8 (STPESANL) tetramer were produced as described previously (36). An Aqua Amine Reactive Dye (AARD) (Invitrogen) was used to exclude dead cells. In some experiments, cells were fixed in 2% paraformaldehyde (PFA) and permeabilized with FACS-perm (BD Bioscience) and stained for Ki-67 and IFN-γ (BD Bioscience). Cells were then fixed with 2% PFA and analyzed by flow cytometry using a 4-laser BD Fortessa instrument (Becton Dickinson). Anti-mouse IgG-coated beads (Invitrogen) were reacted with each fluorochrome-conjugated antibody separately and used for software-based compensation. Cells were analyzed with FlowJo software (TreeStar, Ashland, OR).

T cell stimulation and intracellular cytokine staining (ICS)

T cell stimulation and intracellular cytokine staining were performed similar to a previous detailed description (37). Briefly, 5×10^5 cryopreserved peripheral blood mononuclear cells or lymph node cells were incubated for 1 hour at 37°C in 200 μl of R10 (RPMI-1640 containing 10% bovine growth serum and antibiotics) with anti-CD28, anti-CD49d and 10 μM of the synthetic peptide SIV $Gag_{181-189}$CM9 (CTPYDINQM). Then 10 μg/ml of brefeldin A was added and the cells were incubated an additional 8 hours at 37°C. Cells were then washed in buffer (PBS with 10% serum) and stained for surface expression of CD3, CD4, and CD8 markers and fixed in 2% PFA at 4°C. Cells were then permeabilized in wash buffer containing 1% saponin and stained for expression of the cytokines IFN-γ and TNF-α. Stained cells were acquired on a custom 4 laser BD-Fortessa flow cytometer (Becton Dickinson) with FACSDiva software and analyzed with FlowJo software (TreeStar).

Statistical analyses

Statistical analyses were performed by using GraphPad Prism statistical software (GraphPad Software, San Diego, CA). The Wilcoxon matched-pairs signed rank test and the Mann-Whitney test were performed for comparative statistical analysis. The Spearman's r test was performed for correlation statistical analysis.

RESULTS

Characterization of rhesus macaque Tim-3

To explore the role of Tim-3 in the rhesus macaque model of AIDS, we first determined if Tim-3 was expressed on rhesus cells. The rhesus macaque genome contains a predicted open reading frame with high homology, 79.7%, to human *HAVCR2* (38, 39), and the amino acid sequence also shows high similarity, 87.8%, to human Tim-3 (Figure 1A). Despite the high sequence homology between human and rhesus Tim-3, no antibody reagent has been described that reacts with rhesus Tim-3. Using several commercially available murine and

human monoclonal and polyclonal Tim-3 antibodies, we identified two polyclonal antibodies with cross-reactivity to rhesus macaque PBMC by flow cytometry and western blot analysis (Figure 1B; Supplemental Figure 1). We observed a single band with a molecular weight (MW) of 30 kDa in PMBC derived from both uninfected and SIV-infected animals treated with N-glycosidase F (PNGase F). PBMC derived from an uninfected human subject yielded two bands, one in line with rhesus macaque Tim-3 and an extra band with a MW of 60 kDa. In the absence of PNGase F incubation an increased number of bands were observed suggesting potential modification of Tim-3 by glycosylation (29, 40) (data not shown).

Tim-3$^+$CD8$^+$T cells expand during SIV infection

Using the anti-Tim-3 pAb that gave superior flow staining resolution (Supplemental Figure 1), we first stained rhesus PBMC and examined Tim-3 expression on CD8$^+$ T cells and NK cells. Consistent with our previous observation in humans (41), Tim-3 expression was higher on NK cells than CD8$^+$ T cells, further validating our staining protocol (Supplemental Figure 2). However, Tim-3 expression increases on CD8$^+$ T cells during progressive HIV infection (25). To determine if SIV replication induces similar expansion of Tim-3$^+$CD8$^+$ T cells following SIV infection we compared the levels of Tim-3 on CD8$^+$ T cells in both PBMC and lymph nodes (LN) in uninfected and SIVsmE660 or SIVmac239-infected animals (Supplemental Table 1). Tim-3 expression was greater on CD8$^+$ T cells compared to CD4$^+$ T cells in uninfected animals as has been previously observed in human studies (41, 42) (Figure 1C, D).

We observed that Tim-3 levels on CD8$^+$ T cells from PBMC (Figure 1C) were similar between uninfected and SIV-infected animals. However, the frequency of Tim-3$^+$CD8$^+$ T cells was significantly greater in LN from SIV-infected animals compared to uninfected animals (Figure 1C). This result was independent of the infecting SIV viral strain as no statistically significant difference in the frequency of Tim-3$^+$ CD8$^+$ T cells was observed between SIVsmE660 or SIVmac239 infected animals (data not shown). No significant difference in Tim-3 levels on CD4$^+$ T cells was observed between uninfected and SIV-infected animals in both PBMC and LN (Figure 1D). We also observed a significant increase in LN-derived CD8$^+$ T cells co-expressing Tim-3 and PD-1 in SIV-infected animals (Figure 1E).

Because we observed increased levels of Tim-3 in SIV-infected animals, we next explored the relationship between Tim-3 expression and SIV plasma viremia. LN-derived Tim-3$^+$CD8$^+$ T cells trended towards a positive association with SIV viremia, however this was not statistically significant ($r = 0.42$, $p = 0.08$; Figure 2A). In contrast, LN-derived Tim-3$^+$PD-1$^+$CD8$^+$ T cells positively correlated with SIV plasma viremia ($r = 0.008$, $p = 0.005$; Figure 2C). Neither Tim-3$^+$CD8$^+$ T cells nor Tim-3$^+$PD-1$^+$CD8$^+$ T cells from PBMC were significantly correlated with SIV viremia.

Tim-3 is predominantly expressed on dysfunctional effector memory CD8$^+$ T cells

Effector memory CD8$^+$ T cells are reported to prevent SIV dissemination following acquisition (11-13). We therefore examined the phenotype of Tim-3$^+$ T cells in PBMC, LN

and spleen (19). The greatest representation of Tim-3$^+$ cells was found within the effector memory (CD28$^-$ CD95$^+$) CD8$^+$ T cell compartment with few, if any, cells represented in the naïve (CD28$^+$ CD95$^-$) or central memory T cell (CD28$^+$CD95$^+$) pool in PBMC, LN, or spleens in SIV-infected animals (Figure 3A, B).

We, and others, have previously shown that Tim-3$^+$CD8$^+$ T cells are unable to proliferate and lack cytokine responsiveness to polyclonal or antigen-specific stimulation, indicating that Tim-3 marks dysfunctional CD8$^+$ T cell populations (25, 42). We therefore assessed *ex vivo* co-expression of Tim-3 and the nuclear protein Ki-67, a marker of proliferating cells, in PBMC and LN-derived CD8$^+$ T cells from both SIV-infected and uninfected macaques. Regardless of SIV infection status, most Ki-67$^+$CD8$^+$ T cells lacked Tim-3 expression in both PBMC and LN (Figure 4A). We next examined the IFN-γ response to either mitogenic stimulation with phorbol myristate acetate (PMA) and calcium ionophore ionomycin (Ion) in PBMC from SIV-infected animals or to the immunodominant $Gag_{181\text{-}189}$ CM9 SIV peptide in PBMC from SIV-infected Mamu-A*01+ animals. The production of IFN-γ in response to either PMA+Ion or $Gag_{181\text{-}189}$ CM9 SIV peptide stimulation was principally from Tim-3$^-$ cells**,** especially from $Gag_{181\text{-}189}$ CM9 specific- CD8$^+$ T cells when stimulated with cognate peptide. (Figure 4B, C). These data demonstrate that Tim-3 marks poorly functional effector memory CD8$^+$ T cells in PBMC and LN.

We further examined the expression of Tim-3 on SIV-specific CD8$^+$ T cells by Mamu-A*01:$Gag_{181\text{-}189}$ CM9 tetramer staining. We observed that in PBMC, $Gag_{181\text{-}189}$ CM9-specific CD8$^+$ T cells from chronically SIV-infected animals predominantly lacked Tim-3 expression (Figure 4D). However, Tim-3 expressing $Gag_{181\text{-}189}$CM9-specific CD8$^+$ T cells were present in the secondary lymphoid organs of these animals (Figure 4E). Furthermore, the proportion of Tim-3 expressing cells within the $Gag_{181\text{-}189}$CM9-specific CD8$^+$ T cells were significantly higher in the spleen and lymph nodes in comparison to PMBC (Figure 4F).

Kinetics of Tim-3 expression during acute SIV infection on SIV-specific CD8$^+$ T cells

We previously demonstrated that Tim-3 expression is higher on certain HIV-specific CD8$^+$ T cells (25) and this appears to render high Tim-3 expressing HIV specific T cells vulnerable to regulatory T cell mediated suppression (43). Since Tim-3 expression was lower on $Gag_{181\text{-}189}$ CM9-specific CD8$^+$ T cells in PBMC in chronically SIV-infected macaques, we reasoned that Tim-3 levels may have been downregulated during the acute stage of infection. We therefore assessed the Tim-3 expression kinetics on SIV-specific CD8$^+$ T cells in PBMC from two animals infected with SIVmac239 (Rh24179 and Rh24748) and from two animals infected with SIVmac251 (Rh27002 and Rh28239) during the acute phase of infection using $Gag_{181\text{-}189}$ CM9 and $Tat_{28\text{-}35}$ SL8 tetramers (3). The frequency of $Gag_{181\text{-}189}$ CM9-specific CD8$^+$ T cells showed stable kinetics in all animals through the first 14 weeks of infection (Figure 5A). $Tat_{28\text{-}35}$ SL8-specific CD8$^+$ T cells were present at the highest frequency at 2 weeks post-infection (w.p.i.), but decreased in frequency thereafter. Tim-3 expression peaked on both $Gag_{181\text{-}189}$ CM9 and $Tat_{28\text{-}35}$ SL8-specific CD8$^+$ T cells by 2 w.p.i. and declined thereafter (Figure 5B, C). Both the frequency and MFI of Tim-3 was higher in $Gag_{181\text{-}189}$ CM9-specific CD8$^+$ T cells compared to

Tat_{28-35} SL8-specific $CD8^+$ T cells. We observed that even at this early stage of infection, the frequencies of Ki67 expressing Tim-3+ total or effector memory CD8 T cells was very low compared to Tim-3− cells (Supplemental Figure 3). Interestingly, most $Tim\text{-}3^+CD8^+$ T cells showed high levels of PD-1 expression which is in contrast to PD-1 expression patterns on human HIV-specific CD8 T cells where these levels were much lower (18, 19, 25, 44, 45). We noted, however, that the frequency of $PD\text{-}1^+$ cells were more frequent in both SIV-specific $CD8^+$ T cells than total $CD8^+$ T cells (Figure 5B, D). The mean fluorescence intensity (MFI) of PD-1 was higher on $Gag_{181-189}$ CM9-specific $CD8^+$ T cells compared to Tat_{28-35} SL8-specific $CD8^+$ T cells (Figure 5B, D). Both the frequency and MFI of PD-1 in $Gag_{181-189}$ CM9-specific $CD8^+$ T cells remained high, whereas in Tat_{28-35} SL8-specific $CD8^+$ T cells they declined after 4 w.p.i. (Figure 5B, D) contrasting with Tim-3 kinetics. The Tat_{28-35} SL8 epitope mutates early in infection whereas $Gag_{181-189}$ CM9 epitope is stable or mutates late in infection (46, 47). Consistent with our findings, no viral escape mutations were observed in $Gag_{181-189}$ CM9 in either animal through 14 weeks of infection, but both animals harbored an escape mutation within Tat_{28-35} SL8 by 4 w.p.i (Figure 5E, F). Tim-3 kinetics were not synchronized with viral escape in Tat_{28-35} SL8. However, PD-1 levels declined coincident with Tat_{28-35} SL8 escape. These data suggest PD-1 expression is driven by antigenic stimulation as previously described (19), whereas Tim-3 expression appears to be driven by additional stimuli and is unaffected by viral escape.

DISCUSSION

Negative immune checkpoints are crucial in regulating effector $CD8^+$ T cell responses to chronic viral infections (14-28, 35). The current study was conducted to determine if the Tim-3 pathway is active in nonhuman primates. We demonstrate here, for the first time, the detection of rhesus Tim-3 and provide evidence that rhesus Tim-3 is upregulated in $CD8^+$ T cells derived from secondary lymphoid organs of SIV-infected macaques. $Tim\text{-}3^+CD8^+$ T cells exhibit a predominantly effector memory phenotype and represent a dysfunctional cellular population, suggesting that the Tim-3 pathway is active in the rhesus macaque SIV model of AIDS. Thus, rhesus macaques may represent an appropriate model for interventional studies to improve anti-viral $CD8^+$ T cell responses against chronic pathogens such as SIV.

LN-resident $CD8^+$ T cell responses have recently been shown to predict the efficacy of live-attenuated SIV vaccines (13), supporting the importance of evaluating tissue sites for understanding anti-viral $CD8^+$ T cell activity. Our finding that Tim-3 is increased on LN-derived $CD8^+$ T cells in SIV-infected animals reveals the importance of evaluating secondary lymphoid organs in SIV or HIV patients since viral reservoirs are predominately located within $CD4^+$ T follicular helper cells in LN and in tissue macrophages (48). Several negative immune checkpoint receptors including Tim-3 are found in abundance in the tumor-infiltrating environment compared to those in normal tissues or peripheral blood (49), suggesting that T cell immune dysfunction may be occurring principally within tissue sites. Stationing of SIV-specific effector memory $CD8^+$ T cells at portals of viral entry can potently inhibit the establishment of infection (11). Our findings show effector memory $CD8^+$ T cells from various tissues predominately express Tim-3. Galectin-9 is regarded as a soluble ligand for Tim-3 (29, 50) and is found at high levels in the plasma from patients with

high HIV plasma viremia (51) even during HIV acquisition (52). We propose that LN-derived, SIV-specific Tim-3$^+$CD8$^+$ T cells are rendered dysfunctional through galectin-9-Tim-3 interactions and this may be occurring during the acute phase of infection. It is therefore likely that the transient upregulation of Tim-3 expression in acute infection would lead to the early impairment of SIV-specific effector memory CD8$^+$ T cells. Phosphatidylserine and high-mobility group protein B1 (HMGB1) were also identified as the other ligands for Tim-3, but their functional effects on CD8$^+$ T cells are still largely unknown (53, 54). It is also possible these ligands render CD8$^+$ T cells dysfunctional via Tim-3 ligation.

We observed that $Gag_{181\text{-}189}$ CM9-specific CD8$^+$ T cells expressed higher Tim-3 levels in comparison to $Tat_{28\text{-}35}$ SL8-specific CD8$^+$ T cells during acute SIV infection. When Tim-3 levels were tracked during SIV infection, we observed that Tim-3 levels were unaffected by viral escape mutations contrasting with PD-1 expression levels which tend to decline during escape, as has been previously demonstrated (19). Recent studies further reveal that several of the common gamma-chain cytokines regulate Tim-3 expression on CD8$^+$ T cells independent of antigenic stimulation (41, 54-56). We interpret these results to indicate that persistent Tim-3 expression on virus-specific CD8$^+$ T cells does not require continuous antigenic stimulation.

In chronic HIV infection we, and others, have previously reported variable increases in the levels of Tim-3 expression on different HIV-specific CD8$^+$ T cells (25, 31, 43). Our observation that $Gag_{181\text{-}189}$ CM9-specific CD8$^+$ T cells lacked Tim-3 expression in PBMC from chronically SIV$^+$ primates may suggest that different levels of Tim-3 also occur in different SIV-specific CD8$^+$ T populations. Blockade of Tim-3 by anti-Tim-3 antibody or recombinant Tim-3 reinvigorates CD8$^+$ T cell function (24-26, 32, 50, 55) and may be more effective in reversal of T cell dysfunction compared to other negative inhibitory checkpoints as Tim-3$^+$CD8$^+$ T cells are defective in both cytokine and proliferative capacity in both humans and rhesus macaques.

Recent findings highlight the potential of a dual Tim-3/PD-1 blockade as a potent therapy for improving anti-viral T cell responses. This dual Tim-3/PD-1 blockade substantially suppressed viremia and improved survival in several models of chronic infection (24, 26). The Tim-3$^+$PD-1$^+$CD8$^+$ T cells are not only dysfunctional but also appear to secrete IL-10 in abundance compared to single positive cells in mice (24). Indeed, combination blockade of both of Tim-3 and PD-1 has been shown to substantially improve anti-viral T cell immunity and more importantly suppress viral load (24, 26, 57, 58). Our data demonstrate that Tim-3$^+$PD-1$^+$CD8$^+$ T cells are linked to viral persistence in SIV infection and thus targeting this population with a dual blockade may be more effective at improving anti-viral CD8$^+$ T cell activity than a single Tim-3 or PD-1 blockade alone. During chronic SIV infection, most Tim-3$^+$CD8$^+$ T cells did not co-express PD-1. This might reflect the hierarchical expression and different regulation patterns of these two negative checkpoint molecules. In acute infection the observation that Tim-3 and PD-1 were co-expressed on SIV-specific CD8$^+$ T cells TCR stimulation is known to induce and maintain PD-1 expression. We posit that viral mutations, results in the loss of TCR stimulation in specific CD8$^+$ T cells leading to the downregulation of PD-1 (19), whereas Tim-3 expression

remains stable as a result of its regulation which appears to be induced and maintained by a series of common gamma-chain cytokines (56). Our data suggest prolonged expression of Tim-3 after PD-1 downregulation. The therapeutic efficacy of single or dual blockade of Tim-3 or PD-1 may be relevant and in the timing of intervention to improve or restore anti-SIV T cell immune control.

Assessing the effects of combination antiretroviral therapy (cART) on rhesus Tim-3 expression during SIV infection will be an important next step in our studies since Tim-3 levels in some HIV^+ patients do not decline following suppressive cART (25).

In conclusion, we established a method to detect Tim-3 in rhesus macaques and demonstrate that Tim-3^+CD8^+ T cells are increased after SIV infection, mark dysfunctional T cells, and thus recapitulate Tim-3 characteristics observed in humans and mice. With the management of HIV treatment advocating for the early institution of cART during acute infection (59, 60), our findings suggest that although challenging, this should be supplemented with an immune checkpoint blockade to improve host anti-HIV $CD8^+$ T cell function early during infection. Overall, our findings will aid in our understanding of the Tim-3 pathway in HIV and SIV persistence and afford an opportunity to evaluate pre-clinical targeting of Tim-3 to improve anti-viral and anti-tumor $CD8^+$ T cell immunity.

Supplementary Material

Refer to Web version on PubMed Central for supplementary material.

Acknowledgments

We would like to thank C.Lai, W.Tsai, H.Lin and W.Wang (UH) for critical input in western blot analysis and Dr. Alika Maunakea (UH) for guidance with sequence alignments**.** Elizabeth Seger is a Silver Family Foundation Scholar.

GRANT SUPPORT

The project described was supported in part under Grant award Number AI027757 from the National institutes of Health, NIAID, CFAR and Grant award number P51 OD011092 from the National Center for Research Resources and in part by the Creative and Novel Ideas in HIV Research Program (CNIHR) through a supplement to the University of California San Francisco-Gladstone Institute of Virology & Immunology Center for AIDS Research (UCSF-GIVI CFAR) funding (P30 A1027763) (LCN). This funding was made possible by collaborative efforts of the Office of AIDS Research, the National Institutes of Allergies and Infectious Diseases, and the International AIDS Society. The content is solely the responsibility of the authors and does not necessarily represent the official views of the National Institutes of Health.

Abbreviation used in this article

Ion	Ionomycin
LN	lymph nodes
PBMC	peripheral blood mononuclear cells
PD-1	Programmed Death Receptor 1
PNGase F	Peptide -*N*-Glycosidase F

Tim-3 T cell immunoglobulin- and mucin domain-containing molecule-3

REFERENCES

1. Borrow P, Lewicki H, Hahn BH, Shaw GM, Oldstone MB. Virus-specific CD8+ cytotoxic T-lymphocyte activity associated with control of viremia in primary human immunodeficiency virus type 1 infection. Journal of virology. 1994; 68:6103–6110. [PubMed: 8057491]
2. Brodie SJ, Lewinsohn DA, Patterson BK, Jiyamapa D, Krieger J, Corey L, Greenberg PD, Riddell SR. In vivo migration and function of transferred HIV-1-specific cytotoxic T cells. Nature medicine. 1999; 5:34–41.
3. Goulder PJ, Watkins DI. HIV and SIV CTL escape: implications for vaccine design. Nature reviews. Immunology. 2004; 4:630–640.
4. Jin X, Bauer DE, Tuttleton SE, Lewin S, Gettie A, Blanchard J, Irwin CE, Safrit JT, Mittler J, Weinberger L, Kostrikis LG, Zhang L, Perelson AS, Ho DD. Dramatic rise in plasma viremia after CD8(+) T cell depletion in simian immunodeficiency virus-infected macaques. The Journal of experimental medicine. 1999; 189:991–998. [PubMed: 10075982]
5. Kiepiela P, Ngumbela K, Thobakgale C, Ramduth D, Honeyborne I, Moodley E, Reddy S, de Pierres C, Mncube Z, Mkhwanazi N, Bishop K, van der Stok M, Nair K, Khan N, Crawford H, Payne R, Leslie A, Prado J, Prendergast A, Frater J, McCarthy N, Brander C, Learn GH, Nickle D, Rousseau C, Coovadia H, Mullins JI, Heckerman D, Walker BD, Goulder P. CD8+ T-cell responses to different HIV proteins have discordant associations with viral load. Nature medicine. 2007; 13:46–53.
6. Koup RA, Safrit JT, Cao Y, Andrews CA, McLeod G, Borkowsky W, Farthing C, Ho DD. Temporal association of cellular immune responses with the initial control of viremia in primary human immunodeficiency virus type 1 syndrome. Journal of virology. 1994; 68:4650–4655. [PubMed: 8207839]
7. Liu J, O'Brien KL, Lynch DM, Simmons NL, La Porte A, Riggs AM, Abbink P, Coffey RT, Grandpre LE, Seaman MS, Landucci G, Forthal DN, Montefiori DC, Carville A, Mansfield KG, Havenga MJ, Pau MG, Goudsmit J, H D. Immune control of an SIV challenge by a T-cell-based vaccine in rhesus monkeys. Nature. 2009; 457:87–91. [PubMed: 18997770]
8. Matano T, Shibata R, Siemon C, Connors M, Lane HC, Martin MA. Administration of an anti-CD8 monoclonal antibody interferes with the clearance of chimeric simian/human immunodeficiency virus during primary infections of rhesus macaques. Journal of virology. 1998; 72:164–169. [PubMed: 9420212]
9. Sacha JB, Chung C, Rakasz EG, Spencer SP, Jonas AK, Bean AT, Lee W, Burwitz BJ, Stephany JJ, Loffredo JT, Allison DB, Adnan S, Hoji A, Wilson NA, Friedrich TC, Lifson JD, Yang OO, Watkins DI. Gag-specific CD8+ T lymphocytes recognize infected cells before AIDS-virus integration and viral protein expression. Journal of immunology. 2007; 178:2746–2754.
10. Schmitz JE, Kuroda MJ, Santra S, Sasseville VG, Simon MA, Lifton MA, Racz P, Tenner-Racz K, Dalesandro M, Scallon BJ, Ghrayeb J, Forman MA, Montefiori DC, Rieber EP, Letvin NL, Reimann KA. Control of viremia in simian immunodeficiency virus infection by CD8+ lymphocytes. Science. 1999; 283:857–860. [PubMed: 9933172]
11. Hansen SG, Ford JC, Lewis MS, Ventura AB, Hughes CM, Coyne-Johnson L, Whizin N, Oswald K, Shoemaker R, Swanson T, Legasse AW, Chiuchiolo MJ, Parks CL, Axthelm MK, Nelson JA, Jarvis MA, Piatak M Jr. Lifson JD, Picker LJ. Profound early control of highly pathogenic SIV by an effector memory T-cell vaccine. Nature. 2011; 473:523–527. [PubMed: 21562493]
12. Hansen SG, Vieville C, Whizin N, Coyne-Johnson L, Siess DC, Drummond DD, Legasse AW, Axthelm MK, Oswald K, Trubey CM, Piatak M Jr. Lifson JD, Nelson JA, Jarvis MA, Picker LJ. Effector memory T cell responses are associated with protection of rhesus monkeys from mucosal simian immunodeficiency virus challenge. Nature medicine. 2009; 15:293–299.
13. Fukazawa Y, Park H, Cameron MJ, Lefebvre F, Lum R, Coombes N, Mahyari E, Hagen SI, Bae JY, Iii MD, Swanson T, Legasse AW, Sylwester A, Hansen SG, Smith AT, Stafova P, Shoemaker R, Li Y, Oswald K, Axthelm MK, McDermott A, Ferrari G, Montefiori DC, Edlefsen PT, Piatak

M Jr. Lifson JD, Sekaly RP, Picker LJ. Lymph node T cell responses predict the efficacy of live attenuated SIV vaccines. Nature medicine. 2012

14. Day CL, Kaufmann DE, Kiepiela P, Brown JA, Moodley ES, Reddy S, Mackey EW, Miller JD, Leslie AJ, DePierres C, Mncube Z, Duraiswamy J, Zhu B, Eichbaum Q, Altfeld M, Wherry EJ, Coovadia HM, Goulder PJ, Klenerman P, Ahmed R, Freeman GJ, Walker BD. PD-1 expression on HIV-specific T cells is associated with T-cell exhaustion and disease progression. Nature. 2006; 443:350–354. [PubMed: 16921384]
15. Dyavar Shetty R, Velu V, Titanji K, Bosinger SE, Freeman GJ, Silvestri G, Amara RR. PD-1 blockade during chronic SIV infection reduces hyperimmune activation and microbial translocation in rhesus macaques. The Journal of clinical investigation. 2012; 122:1712–1716. [PubMed: 22523065]
16. Hafler DA, Kuchroo V. TIMs: central regulators of immune responses. The Journal of experimental medicine. 2008; 205:2699–2701. [PubMed: 19015312]
17. Vali B, Yue FY, Jones RB, Sheth PM, Kaul R, Betts MR, Wong D, Kovacs C, Loutfy M, Common A, Halpenny R, Ostrowski MA. HIV-specific T-cells accumulate in the liver in HCV/HIV co-infection. PloS one. 2008; 3:e3454. [PubMed: 18941622]
18. Petrovas C, Casazza JP, Brenchley JM, Price DA, Gostick E, Adams WC, Precopio ML, Schacker T, Roederer M, Douek DC, Koup RA. PD-1 is a regulator of virus-specific CD8+ T cell survival in HIV infection. The Journal of experimental medicine. 2006; 203:2281–2292. [PubMed: 16954372]
19. Petrovas C, Price DA, Mattapallil J, Ambrozak DR, Geldmacher C, Cecchinato V, Vaccari M, Tryniszewska E, Gostick E, Roederer M, Douek DC, Morgan SH, Davis SJ, Franchini G, Koup RA. SIV-specific CD8+ T cells express high levels of PD1 and cytokines but have impaired proliferative capacity in acute and chronic SIVmac251 infection. Blood. 2007; 110:928–936. [PubMed: 17440051]
20. Porichis F, Kaufmann DE. Role of PD-1 in HIV pathogenesis and as target for therapy. Curr HIV/AIDS Rep. 2012; 9:81–90. [PubMed: 22198819]
21. Trautmann L, Janbazian L, Chomont N, Said EA, Gimmig S, Bessette B, Boulassel MR, Delwart E, Sepulveda H, Balderas RS, Routy JP, Haddad EK, Sekaly RP. Upregulation of PD-1 expression on HIV-specific CD8+ T cells leads to reversible immune dysfunction. Nature medicine. 2006; 12:1198–1202.
22. Velu V, Titanji K, Zhu B, Husain S, Pladevega A, Lai L, Vanderford TH, Chennareddi L, Silvestri G, Freeman GJ, Ahmed R, Amara RR. Enhancing SIV-specific immunity in vivo by PD-1 blockade. Nature. 2009; 458:206–210. [PubMed: 19078956]
23. Wherry EJ. T cell exhaustion. Nat Immunol. 2011; 12:492–499. [PubMed: 21739672]
24. Jin HT, Anderson AC, Tan WG, West EE, Ha SJ, Araki K, Freeman GJ, Kuchroo VK, Ahmed R. Cooperation of Tim-3 and PD-1 in CD8 T-cell exhaustion during chronic viral infection. Proceedings of the National Academy of Sciences of the United States of America. 2010; 107:14733–14738. [PubMed: 20679213]
25. Jones RB, Ndhlovu LC, Barbour JD, Sheth PM, Jha AR, Long BR, Wong JC, Satkunarajah M, Schweneker M, Chapman JM, Gyenes G, Vali B, Hyrcza MD, Yue FY, Kovacs C, Sassi A, Loutfy M, Halpenny R, Persad D, Spotts G, Hecht FM, Chun TW, McCune JM, Kaul R, Rini JM, Nixon DF, Ostrowski MA. Tim-3 expression defines a novel population of dysfunctional T cells with highly elevated frequencies in progressive HIV-1 infection. The Journal of experimental medicine. 2008; 205:2763–2779. [PubMed: 19001139]
26. McMahan RH, Golden-Mason L, Nishimura MI, McMahon BJ, Kemper M, Allen TM, Gretch DR, Rosen HR. Tim-3 expression on PD-1+ HCV-specific human CTLs is associated with viral persistence, and its blockade restores hepatocyte-directed in vitro cytotoxicity. The Journal of clinical investigation. 2010; 120:4546–4557. [PubMed: 21084749]
27. Nebbia G, Peppa D, Schurich A, Khanna P, Singh HD, Cheng Y, Rosenberg W, Dusheiko G, Gilson R, ChinAleong J, Kennedy P, Maini MK. Upregulation of the Tim-3/galectin-9 pathway of T cell exhaustion in chronic hepatitis B virus infection. PloS one. 2012; 7:e47648. [PubMed: 23112829]

28. Takamura S, Tsuji-Kawahara S, Yagita H, Akiba H, Sakamoto M, Chikaishi T, Kato M, Miyazawa M. Premature terminal exhaustion of Friend virus-specific effector CD8+ T cells by rapid induction of multiple inhibitory receptors. Journal of immunology. 2010; 184:4696–4707.
29. Zhu C, Anderson AC, Schubart A, Xiong H, Imitola J, Khoury SJ, Zheng XX, Strom TB, Kuchroo VK. The Tim-3 ligand galectin-9 negatively regulates T helper type 1 immunity. Nat Immunol. 2005; 6:1245–1252. [PubMed: 16286920]
30. Tandon R, Giret MT, Sengupta D, York VA, Wiznia AA, Rosenberg MG, Kallas EG, Ndhlovu LC, Nixon DF. Age-related expansion of Tim-3 expressing T cells in vertically HIV-1 infected children. PloS one. 2012; 7:e45733. [PubMed: 23029209]
31. Kassu A, Marcus RA, D'Souza MB, Kelly-McKnight EA, Palmer BE. Suppression of HIV replication by antiretroviral therapy reduces TIM-3 expression on HIV-specific CD8(+) T cells. AIDS research and human retroviruses. 2011; 27:1–3. [PubMed: 20860535]
32. Golden-Mason L, Palmer BE, Kassam N, Townshend-Bulson L, Livingston S, McMahon BJ, Castelblanco N, Kuchroo V, Gretch DR, Rosen HR. Negative immune regulator Tim-3 is overexpressed on T cells in hepatitis C virus infection and its blockade rescues dysfunctional CD4+ and CD8+ T cells. Journal of virology. 2009; 83:9122–9130. [PubMed: 19587053]
33. Schietinger A, Greenberg PD. Tolerance and exhaustion: defining mechanisms of T cell dysfunction. Trends in immunology. 2013
34. Crespo J, Sun H, Welling TH, Tian Z, Zou W. T cell anergy, exhaustion, senescence, and stemness in the tumor microenvironment. Current opinion in immunology. 2013; 25:214–221. [PubMed: 23298609]
35. Sakhdari A, Mujib S, Vali B, Yue FY, MacParland S, Clayton K, Jones RB, Liu J, Lee EY, Benko E, Kovacs C, Gommerman J, Kaul R, Ostrowski MA. Tim-3 negatively regulates cytotoxicity in exhausted CD8+ T cells in HIV infection. PloS one. 2012; 7:e40146. [PubMed: 22792231]
36. Mothe BR, Horton H, Carter DK, Allen TM, Liebl ME, Skinner P, Vogel TU, Fuenger S, Vielhuber K, Rehrauer W, Wilson N, Franchini G, Altman JD, Haase A, Picker LJ, Allison DB, Watkins DI. Dominance of CD8 responses specific for epitopes bound by a single major histocompatibility complex class I molecule during the acute phase of viral infection. Journal of virology. 2002; 76:875–884. [PubMed: 11752176]
37. Vogel TU, Friedrich TC, O'Connor DH, Rehrauer W, Dodds EJ, Hickman H, Hildebrand W, Sidney J, Sette A, Hughes A, Horton H, Vielhuber K, Rudersdorf R, De Souza IP, Reynolds MR, Allen TM, Wilson N, Watkins DI. Escape in one of two cytotoxic T-lymphocyte epitopes bound by a high-frequency major histocompatibility complex class I molecule, Mamu-A*02: a paradigm for virus evolution and persistence? Journal of virology. 2002; 76:11623–11636. [PubMed: 12388723]
38. Okagawa T, Konnai S, Ikebuchi R, Suzuki S, Shirai T, Sunden Y, Onuma M, Murata S, Ohashi K. Increased bovine Tim-3 and its ligand expressions during bovine leukemia virus infection. Veterinary research. 2012; 43:45. [PubMed: 22621175]
39. Yan G, Zhang G, Fang X, Zhang Y, Li C, Ling F, Cooper DN, Li Q, Li Y, van Gool AJ, Du H, Chen J, Chen R, Zhang P, Huang Z, Thompson JR, Meng Y, Bai Y, Wang J, Zhuo M, Wang T, Huang Y, Wei L, Li J, Wang Z, Hu H, Yang P, Le L, Stenson PD, Li B, Liu X, Ball EV, An N, Huang Q, Zhang Y, Fan W, Zhang X, Li Y, Wang W, Katze MG, Su B, Nielsen R, Yang H, Wang J, Wang X, Wang J. Genome sequencing and comparison of two nonhuman primate animal models, the cynomolgus and Chinese rhesus macaques. Nat Biotechnol. 2011; 29:1019–1023. [PubMed: 22002653]
40. Kuchroo VK, Umetsu DT, DeKruyff RH, Freeman GJ. The TIM gene family: emerging roles in immunity and disease. Nature reviews. Immunology. 2003; 3:454–462.
41. Ndhlovu LC, Lopez-Verges S, Barbour JD, Jones RB, Jha AR, Long BR, Schoeffler EC, Fujita T, Nixon DF, Lanier LL. Tim-3 marks human natural killer cell maturation and suppresses cell-mediated cytotoxicity. Blood. 2012; 119:3734–3743. [PubMed: 22383801]
42. Hastings WD, Anderson DE, Kassam N, Koguchi K, Greenfield EA, Kent SC, Zheng XX, Strom TB, Hafler DA, Kuchroo VK. TIM-3 is expressed on activated human CD4+ T cells and regulates Th1 and Th17 cytokines. European journal of immunology. 2009; 39:2492–2501. [PubMed: 19676072]

43. Elahi S, Dinges WL, Lejarcegui N, Laing KJ, Collier AC, Koelle DM, McElrath MJ, Horton H. Protective HIV-specific CD8+ T cells evade Treg cell suppression. Nature medicine. 2011; 17:989–995.
44. Youngblood B, Noto A, Porichis F, Akondy RS, Ndhlovu ZM, Austin JW, Bordi R, Procopio FA, Miura T, Allen TM, Sidney J, Sette A, Walker BD, Ahmed R, Boss JM, Sekaly RP, Kaufmann DE. Cutting edge: Prolonged exposure to HIV reinforces a poised epigenetic program for PD-1 expression in virus-specific CD8 T cells. Journal of immunology. 2013; 191:540–544.
45. Xu H, Wang X, Lackner AA, Veazey RS. CD8 down-regulation and functional impairment of SIV-specific cytotoxic T lymphocytes in lymphoid and mucosal tissues during SIV infection. Journal of leukocyte biology. 2013; 93:943–950. [PubMed: 23519937]
46. Bimber BN, Burwitz BJ, O'Connor S, Detmer A, Gostick E, Lank SM, Price DA, Hughes A, O'Connor D. Ultradeep pyrosequencing detects complex patterns of CD8+ T-lymphocyte escape in simian immunodeficiency virus-infected macaques. Journal of virology. 2009; 83:8247–8253. [PubMed: 19515775]
47. Burwitz BJ, Sacha JB, Reed JS, Newman LP, Norante FA, Bimber BN, Wilson NA, Watkins DI, O'Connor DH. Pyrosequencing reveals restricted patterns of CD8+ T cell escape-associated compensatory mutations in simian immunodeficiency virus. Journal of virology. 2011; 85:13088–13096. [PubMed: 21994463]
48. Perreau M, Savoye AL, De Crignis E, Corpataux JM, Cubas R, Haddad EK, De Leval L, Graziosi C, Pantaleo G. Follicular helper T cells serve as the major CD4 T cell compartment for HIV-1 infection, replication, and production. The Journal of experimental medicine. 2013; 210:143–156. [PubMed: 23254284]
49. Gao X, Zhu Y, Li G, Huang H, Zhang G, Wang F, Sun J, Yang Q, Zhang X, Lu B. TIM-3 expression characterizes regulatory T cells in tumor tissues and is associated with lung cancer progression. PloS one. 2012; 7:e30676. [PubMed: 22363469]
50. Sehrawat S, Reddy PB, Rajasagi N, Suryawanshi A, Hirashima M, Rouse BT. Galectin-9/TIM-3 interaction regulates virus-specific primary and memory CD8 T cell response. PLoS pathogens. 2010; 6:e1000882. [PubMed: 20463811]
51. Saitoh H, Ashino Y, Chagan-Yasutan H, Niki T, Hirashima M, Hattori T. Rapid decrease of plasma galectin-9 levels in patients with acute HIV infection after therapy. The Tohoku journal of experimental medicine. 2012; 228:157–161. [PubMed: 23038209]
52. Tandon R, Chew GM, Byron MM, Borrow P, Niki T, Hirashima M, Barbour JD, Norris PJ, Lanteri MC, Martin JN, Deeks SG, Ndhlovu LC. Galectin-9 is rapidly released during acute HIV-1 infection and remains sustained at high levels despite viral suppression even in elite controllers. AIDS research and human retroviruses. 2014; 30:654–664. [PubMed: 24786365]
53. Freeman GJ, Casasnovas JM, Umetsu DT, DeKruyff RH. TIM genes: a family of cell surface phosphatidylserine receptors that regulate innate and adaptive immunity. Immunological reviews. 2010; 235:172–189. [PubMed: 20536563]
54. Chiba S, Baghdadi M, Akiba H, Yoshiyama H, Kinoshita I, Dosaka-Akita H, Fujioka Y, Ohba Y, Gorman JV, Colgan JD, Hirashima M, Uede T, Takaoka A, Yagita H, Jinushi M. Tumor-infiltrating DCs suppress nucleic acid-mediated innate immune responses through interactions between the receptor TIM-3 and the alarmin HMGB1. Nat Immunol. 2012; 13:832–842. [PubMed: 22842346]
55. Yang ZZ, Grote DM, Ziesmer SC, Niki T, Hirashima M, Novak AJ, Witzig TE, Ansell SM. IL-12 upregulates TIM-3 expression and induces T cell exhaustion in patients with follicular B cell non-Hodgkin lymphoma. The Journal of clinical investigation. 2012; 122:1271–1282. [PubMed: 22426209]
56. Mujib S, Jones RB, Lo C, Aidarus N, Clayton K, Sakhdari A, Benko E, Kovacs C, Ostrowski MA. Antigen-independent induction of Tim-3 expression on human T cells by the common gamma-chain cytokines IL-2, IL-7, IL-15, and IL-21 is associated with proliferation and is dependent on the phosphoinositide 3-kinase pathway. Journal of immunology. 2012; 188:3745–3756.
57. Li W, Green WR. Immunotherapy of murine retrovirus-induced acquired immunodeficiency by CD4 T regulatory cell depletion and PD-1 blockade. Journal of virology. 2011; 85:13342–13353. [PubMed: 21917983]

58. Dietze KK, Zelinskyy G, Liu J, Kretzmer F, Schimmer S, Dittmer U. Combining regulatory T cell depletion and inhibitory receptor blockade improves reactivation of exhausted virus-specific CD8(+) T cells and efficiently reduces chronic retroviral loads. PLoS pathogens. 2013; 9:e1003798. [PubMed: 24339778]

59. Stekler JD, Wellman R, Holte S, Maenza J, Stevens CE, Corey L, Collier AC. Are there benefits to starting antiretroviral therapy during primary HIV infection? Conclusions from the Seattle Primary Infection Cohort vary by control group. International journal of STD & AIDS. 2012; 23:201–206. [PubMed: 22581875]

60. Evering TH, Mehandru S, Racz P, Tenner-Racz K, Poles MA, Figueroa A, Mohri H, Markowitz M. Absence of HIV-1 evolution in the gut-associated lymphoid tissue from patients on combination antiviral therapy initiated during primary infection. PLoS pathogens. 2012; 8:e1002506. [PubMed: 22319447]

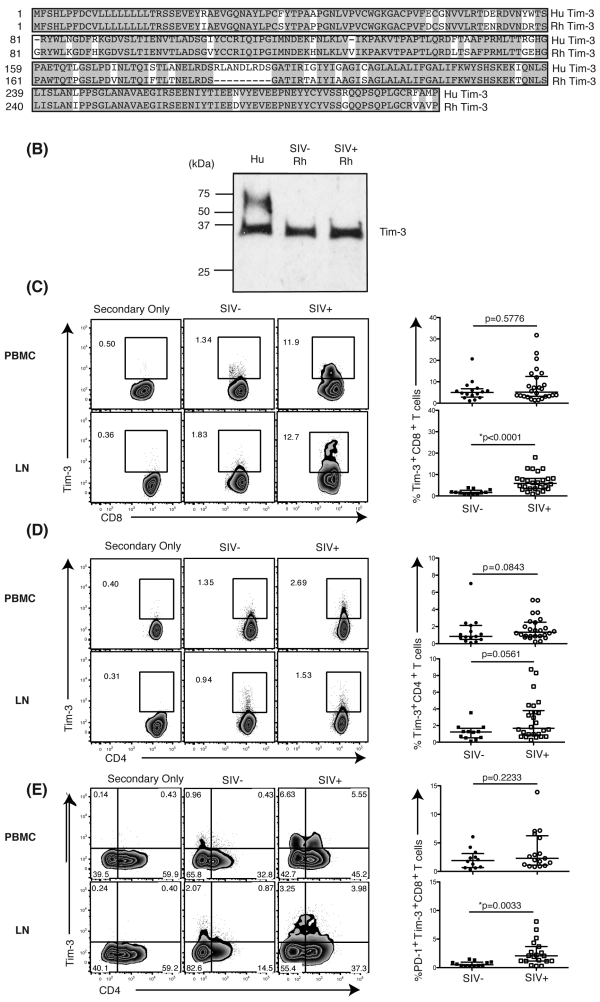

Figure 1. Detection and expression of Rhesus Tim-3 in T cells derived from blood and lymph nodes

(A) Alignment shows amino acid sequences of human Tim-3 (Hu Tim-3) and rhesus Tim-3 (Rh Tim-3). Highlighted sequences indicate homology between human and rhesus Tim-3. Dashes indicate gaps in alignment. (B) Bands are blotted with polyclonal anti-human Tim-3 antibody from R&D. Hu: human, Rh: rhesus, SIV-: SIV-uninfected, SIV+: SIV-infected. (C) Flow plots depict the Tim-3 expression on $CD8^+$ T cells from PBMC and LN in SIV-uninfected and SIV-infected animals in a representative animal. Graphs show the frequency [%] of $Tim\text{-}3^+CD8^+$ T cells from PBMC (circle) and LN (square) in SIV-uninfected (solid) and SIV-infected (open) animals. SIV-uninfected PBMC: n=16, SIV-infected PBMC: n=26, SIV-uninfected LN: n=12, SIV-infected LN: n=26. (D) Flow plots depict the Tim-3 expression on $CD4^+$ T cells from PBMC and LN in SIV-uninfected and SIV-infected animals in a representative animal. Graphs show the frequency [%] of $Tim\text{-}3^+CD4^+$ T cells from PBMC (circle) and LN (square) in SIV-uninfected (solid) and SIV-infected (open) animals. SIV-uninfected PBMC: n=16, SIV-infected PBMC: n=26, SIV-uninfected LN: n=12, SIV-infected LN: n=26. (E) Flow plots depict the Tim-3 and PD-1 co-expression on $CD8^+$ T cells from PBMC and LN in representative SIV-uninfected and SIV-infected animals. Graphs show the frequency [%] of $Tim\text{-}3^+PD\text{-}1^+CD8^+$ T cells from PBMC and LN

in SIV-uninfected and SIV-infected animals. SIV-uninfected PBMC: n=12, SIV-infected PBMC: n=17, SIV-uninfected LN: n=12, SIV-infected LN: n=20. A Mann-Whitney test was performed for statistical analysis. Control cells were stained with the secondary antibodies without using the anti-Tim-3 primary antibody. Both SIVsmE660 and SIVmac239 infected macaques were used for these analyses.

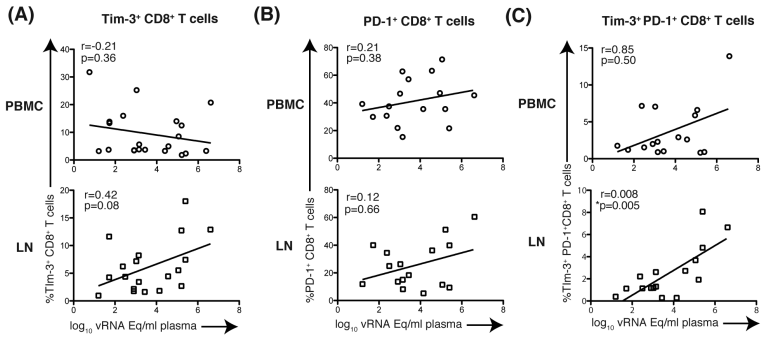

Figure 2. Correlation of Tim-3 expressing CD8$^+$ T cells and plasma SIV Viral load

(A) Graphs show correlation of plasma SIVsmE660 viral load and frequency of Tim-3$^+$CD8$^+$ T cells from PBMC and LN. PBMC: n=20, LN: n=19. (B) Graphs show correlation of plasma SIV smE660 viral load and frequency of Tim-3$^+$CD8$^+$ T cells from PBMC and LN. PBMC: n=16, LN: n=16. (C) Graphs show correlation of plasma SIV smE660 viral load and frequency of Tim-3$^+$PD-1$^+$CD8$^+$ T cells from PBMC and LNs. PBMC:n=16, LN: n=16. A Spearman's r test was performed for statistical analysis. vRNA Eq: viral RNA copy equivalents. All data points for SIVsmE660 vRNA and Tim-3 expression levels are from the same samples (plasma and PBMC, respectively) taken from the same time point.

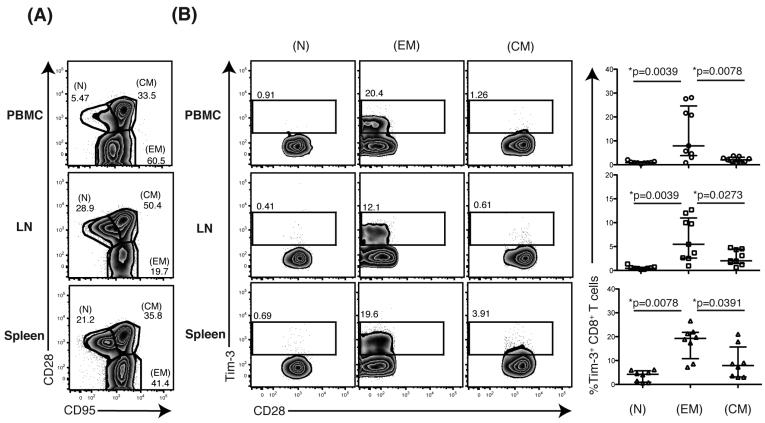

Figure 3. Phenotypic assessment of rhesus Tim-3 expressing CD8$^+$ T cells in various tissues

(A) Flow plots show the gating of naïve (CD28$^+$CD95$^-$) (N), effector memory (CD28$^-$CD95$^+$) (EM), and central memory (CD28$^+$CD95$^+$) (CM) CD8$^+$ T cells from SIV-infected PBMC, LN or spleen in a representative animal. (B) Flow plots depict the Tim-3 expression on N, EM and CM CD8$^+$ T cells from PBMC, LN, or spleen in a representative SIVsmE660-infected animal. Graphs show the frequency [%] of Tim-3$^+$ N, EM and CM CD8$^+$ T cells from SIV-infected PBMC, LN or spleen. PBMC: n=9, LN: n=9, spleen: n=8. A Wilcoxon matched-pairs signed rank test was performed for statistical analysis.

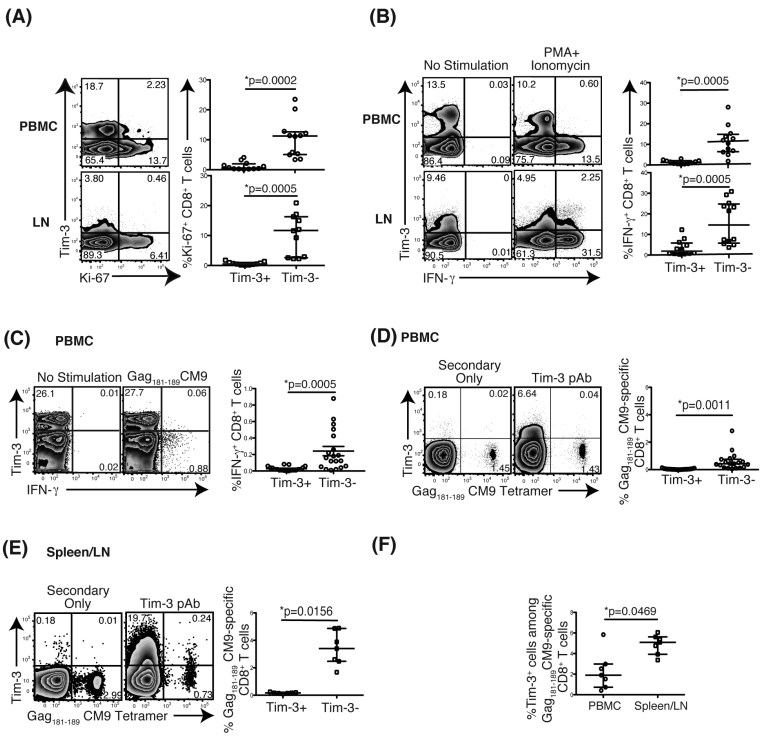

Figure 4. Tim-3-expressing CD8$^+$ T cells have impaired proliferative capacity and cytokine responses

(A) Flow plots depict representative Ki-67 and Tim-3 expression in PBMC and LN. Graphs show the frequency [%] of Tim-3$^+$Ki-67$^+$ and Tim-3$^-$Ki-67$^+$ CD8$^+$ T cells in PBMC and LN. Cells from both SIV-naïve and SIV-infected animals were used. PBMC: n=12, LN: n=11. (B) Flow plots depict representative IFN-γ and Tim-3 expression in PBMC and LN from SIV-infected animals. Graphs show the frequency [%] of Tim-3$^+$IFN-γ$^+$ and Tim-3$^-$IFN-γ$^+$ CD8$^+$ T cells in PBMC and LN from SIV-infected animals following mitogen stimulation. PBMC: n=12, LN: n=12. (C) Flow plots depict IFN-γ and Tim-3 expression in CD8$^+$ T cells from PBMC without or with $Gag_{181\text{-}189}$ CM9 peptide stimulation in a representative Mamu-A01+ animal. Graphs show the frequency [%] of Tim-3$^+$IFN-γ$^+$ and Tim-3$^-$IFN-γ$^+$ CD8$^+$ T cells in PBMC from Mamu-A01+ SIV-infected animals. n=14. (D) Flow plots depict the Tim-3 expression on $Gag_{181\text{-}189}$ CM9-specific CD8$^+$ T cells stained with CM9 tetramer in a representative animal. A Graph shows the frequency [%] of Tim-3$^-$ and Tim-3$^+$ $Gag_{181\text{-}189}$ CM9-specific CD8$^+$ T cells in PBMC from SIV-infected animals. n=14. (E) Flow plots represent Tim-3 expressing $Gag_{181\text{-}189}$ CM9-specific CD8$^+$ T cells in secondary lymphoid tissues derived from LN and spleen in Mamu-A01+ SIVsmE660 and SIVmac239/251 infected animals. (F) Graph depicts the comparisons between the frequency of Tim-3 expressing $Gag_{181\text{-}189}$ CM9-specific CD8$^+$ T cells in PBMC and in secondary lymphoid tissues. Control cells were stained with the secondary antibodies without using the anti-Tim-3 primary antibody. A Wilcoxon matched-pairs signed rank test was performed for statistical analysis.

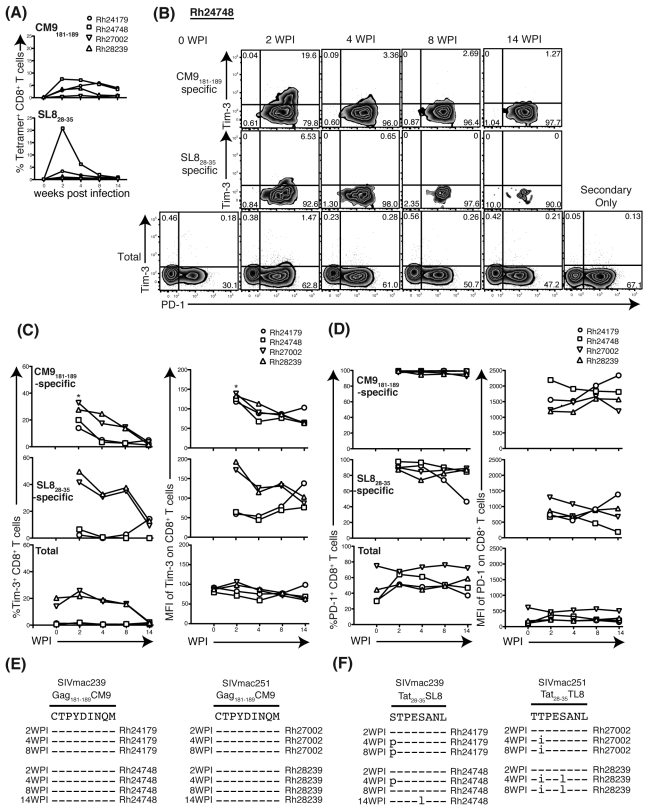

Figure 5. Kinetics of Tim-3 and PD-1 expression on SIV-specific CD8$^+$ T cells during acute SIV infection

(A) Graphs show the change of frequency [%] of $Gag_{181\text{-}189}$ CM9 or $Tat_{28\text{-}35}$ SL8-specific CD8$^+$ T cells in four animals, Rh24179 (circle), Rh24748 (square), Rh27002 (reverse triangle) and Rh28239 (triangle). (B) Flow plots show the change of Tim-3 and PD-1 on $Gag_{181\text{-}189}$ CM9-specific, $Tat_{28\text{-}35}$ SL8-specific or total CD8$^+$ T cells in a representative animal (Rh24748) (C) Graphs show change of frequency [%] (left) and MFI (right) of Tim-3 in $Gag_{181\text{-}189}$ CM9-specific, $Tat_{28\text{-}35}$ SL8-specific or total CD8$^+$ T cells in two animals. (D) Graphs show change of frequency [%] (left) and MFI (right) of PD-1 in $Gag_{181\text{-}189}$ CM9-specific, $Tat_{28\text{-}35}$ SL8-specific or total CD8$^+$ T cells in two animals. (E) Alignment shows SIV genome sequence of CM9 region in each time points. Dashed lines indicate sequence identity. (F) Alignment shows SIV genome sequence of SL8 region in each time points. Dashes indicate identity to the sequence. WPI: weeks post infection. Control cells were stained with the secondary antibodies without using the anti-Tim-3 primary antibody.